Impact fracture of a three-dimensional cube with quenched disorder

Jan Åström and Jussi Timonen
Department of Physics, University of Jyväskylä, P.O. Box 35, FIN-40351 Jyväskylä, Finland
(Received 4 January 1999)

Disorder is demonstrated to be a decisive factor that controls the location and the amount of damage caused by a rapid impact on a three-dimensional elastic solid. For strong disorder, the damage is localized close to the point of impact, while for weak disorder, constructive interference leads to fracture in the vicinity of the face opposite to the impact. Dynamical overload seems to hinder the formation of self-affine crack structures. However, the crack surface becomes more rough as the quasistatic limit is approached.
[S1063-651X(99)08104-0]

PACS number(s): 46.50.+a

In addition to their great technological importance, impact fracture and fragmentation processes are also interesting from a purely academic point of view. The academic interest relates to many basic aspects of fracture and fragmentation not being fully understood, even though such processes are common in everyday life. The difficulties related to dynamic fracture are, as in quasistatic fracture, a consequence of the average properties of a material not being enough to determine its failure behavior. Rather, fracture processes are determined by weaknesses and microcracks (i.e., disorder) which exist in all natural materials [1]. Fragmentation is usually initiated at such weaknesses, and interaction between them and nucleated cracks will influence the dynamic fracture process in a highly nontrivial way [2,3]. Attempts to relate fragmentation and fracture to self-organized criticality and phase transitions have appeared recently [4,5]. There are also a few more or less simplified models which catch many of the features typical of dynamic fracture and fragmentation [2,3,6–8]. The picture is still far from being complete, however.

In this paper we analyze dynamic fracture by a rapid impact of a discrete lattice model of a three-dimensional cube. We shall not quantitatively consider any specific process, but rather consider a numerically efficient model in order to extract qualitative effects of statistical disorder in three-dimensional impact fracture (for reviews of fracture in two dimensions, see, e.g., Refs. [9, 10]). Similarly to the finite-element method, we divide the solid body into discrete lattice sites and bonds. For numerical reasons we have chosen to use a simple cubic lattice. All mass is lumped into the sites, and a harmonic potential is assumed between nearest neighbor sites. The displacements and accelerations of all sites are computed at discrete time steps. The harmonic potential in the six-dimensional local phase space (i.e., three translational and three rotational degrees of freedom for each site) is taken to be that of a slender, linearly elastic, beam (so slender that shear deformations are negligible in comparison with bending). The boundary conditions imposed on the lattice cube are chosen such that the sites at the bottom face of the cube ($z=0$) are time dependent: $z(t)=A\sin^2(\omega t)$ for $0 \leqslant t \leqslant \pi/2\omega$. For $t>\pi/2\omega$, these sites are forced to stay at $z=A$. This dependence models the impact. Free boundary conditions are imposed on all other faces of the cube. The time-dependent displacements of all sites other than those on the bottom face are computed using a discrete form of Newton's equations of motion including a small linear viscous dissipation term, and starting from the global static equilibrium at $t=0$. The equations of motion are

$$\left[\frac{M}{\Delta t^2}+\frac{C}{2\Delta t}\right]U(t+\Delta t) = \left[\frac{2M}{\Delta t^2}-K\right]U(t)-\left[\frac{M}{\Delta t^2}-\frac{C}{2\Delta t}\right]U(t-\Delta t), \quad (1)$$

where M is the diagonal mass matrix, K the stiffness matrix, C a diagonal damping matrix, U a vector containing the displacements from equilibrium of all lattice sites, and Δt the length of the discrete time step. In the simulations M and C are both set proportional to the unit matrix, and $U(0)=U(-\Delta t)=0$; K is constructed by summing the stiffness matrices of all lattice bonds [11]. For maximizing the numerical efficiency we do not upgrade K as the cube is being deformed. This means that, in a strict sense, our model is only correct for infinitesimal displacements. Fracture, being a local process, is introduced on the smallest possible scale in the model, i.e., on the scale of a single bond. A lattice bond will break instantly and irreversibly if its axial elongation or compression exceeds given threshold values. For simplicity, it is not possible to break a bond by bending. Notice, however, that a global bending of the cube can cause fracture. To test the effect of the lattice geometry we used two different propagation directions for the compression wave (the [100] and [111] directions). The propagation direction is important because cracks can only propagate perpendicularly to lattice bonds.

Disorder could be introduced in many ways. We have chosen to use random distributions for the masses at the lattice sites and for the Young's moduli of the bonds. The masses m_i (also the moments of inertia) and the Young's moduli E_i are chosen from exponential distributions: $m_i=a^{\delta_i}$ and $E_i=a^{\gamma_i}$, where δ_i and γ_i are stochastic variables whose values are uncorrelated and belong to the uniform distribution in the interval [0, 1]. Here a is the ''width'' of these distributions. Notice that if damping is negligible, the *averaged* dynamical properties of the system remain the

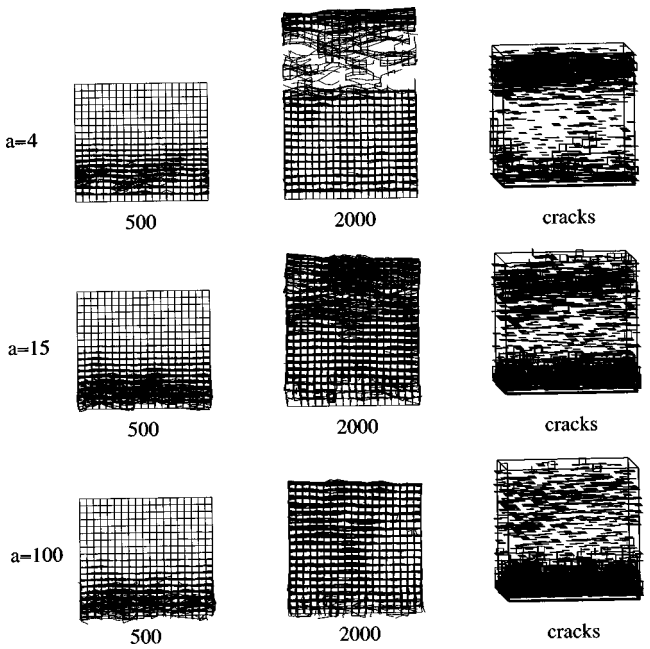

FIG. 1. Snapshots of three fragmentation processes at 500 and 2000 time steps ($\Delta t = 0.05$). $a = 4$, 15, and 100. The cracks formed after 2000 time steps are also shown.

same even if a is changed [cf. Eq. (1)]. It is only the amplitude of the local fluctuations that would change, i.e., disorder.

In Fig. 1 we show snapshots taken from one face of the lattice cube (so that it appears two dimensional) at early and late stages of the fracture processes, and for three different values of a. In this figure we also display the cracks which are formed. In the simulations the following parameters were used: beam cross section $\omega^2 = 0.25$, beam length $l_f = 1.0$, lattice size $20 \times 20 \times 20$, and $\omega = \pi/40$. The compressive fracture threshold was $0.25 l_f$, and the tensile fracture threshold $0.05 l_f$. After 500 time steps ($\Delta t = 0.05$) and for $a = 4$, a compression wave is clearly seen. For $a = 15$, and especially for $a = 100$, severe fragmentation close to the point of impact can already be observed after 500 time steps. This has caused a decreased amplitude of the compression wave as elastic energy is absorbed by and reflected from nucleating cracks. The average maximum displacement of the sites halfway through the cube was $1.2A$ for $a = 4$, and $0.5A$ for $a = 100$. After 2000 time steps the compression wave has already traveled back and forth through the cube. In the case when $a = 4$, the first time the wave reaches the opposite face of the cube, a positive interference between the coming and the reflected wave results in fracture close to this face. The cracks formed for $a = 4$ are thus concentrated near the face opposite to the impact. For $a = 15$ cracks are formed at both ends of the cube, while for $a = 100$ the cracks are concentrated in the vicinity of the impact. Notice that the values of the tensile and the compressive fracture thresholds are very important. If the compressive fracture threshold is very small, many bonds will break before the maximum of the wave has passed that point. This means that a lot of elastic energy is arrested behind the cracks. If, on the other hand, most bonds are broken by tensile stress, elastic energy propagates more easily.

Figure 2 demonstrates, in a more quantitative form, the

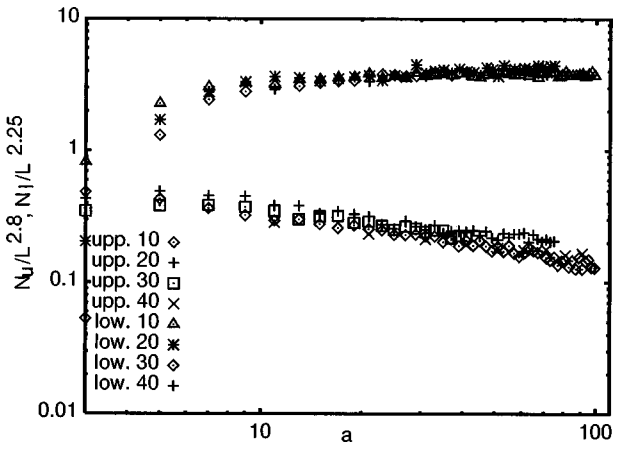

FIG. 2. The number of broken bonds in the upper (N_u) and the lower (N_l) halves, scaled by a power of the linear size (L) of the cube, and plotted as functions of a. Results are shown for $L = 10$, 20, 30, and 40.

change in the number of broken bonds with the increase of disorder. In this figure we show the number of broken bonds (scaled by a power of the cube size L) in the upper and lower halves of the cube as functions of a. In the upper half the number of broken bonds decreases with increasing a, while it increases in the lower half.

The dimensionality of the cracks formed in the vicinity of the bottom and top faces of the cubes is not clear from Fig. 1. The dimensions of these structures can be obtained by doing simulations on different cube sizes and then collapsing the curves, like the ones in Fig. 2, onto a single curve by scaling the y axis by $L^{-\delta}$, where δ is the dimension. This has been done in Fig. 2. The best result for the lower cracks is given by $\delta \approx 2.25$, and for the upper cracks $\delta \approx 2.8$. If this collapsing of the curves is perfect, it would indicate that the cracks form self-affine structures with the fractal dimension δ. This is the case for quasistatic fracture [12–15]. However, there seems to be a weakly decreasing trend in δ with increasing L. This indicates that the structures formed by the cracks are not really scale invariant, and that there may be a crossover size at which the dimensions change. This is indeed the case as demonstrated by Fig. 3(A) for the upper cracks, and by Fig. 3(B) for the lower cracks. The number of broken bonds in the respective halves of the cube are plotted as functions of the linear system size L for $a = 5$, 13, 51, and 200. Figures 3(A) and 3(B) demonstrate that the crack structures are close to three dimensional on a small scale, and close to two dimensional on a large scale for both the upper and the lower cracks. That is, the fracture zones have the structure of a plate of finite thickness. Notice also that the crossover point from three to two dimensions is disorder dependent for the (100) direction, while it seems independent of disorder for the (111) direction. The above result is in contrast to what is found for the quasistatic case. In two dimensions the exponent 1.7 appears for all types of disorder [12], unless the disorder distribution is very narrow. In three dimensions the exponents 2.25 and 2.9 were reported for weak and strong disorder, respectively, in a cubic fuse lattice with uniformly distributed fracture thresholds [13]. The exponents 2.1 and 2.6 were also reported in three dimensions for slightly different types of disorder and lattice geometry [14].

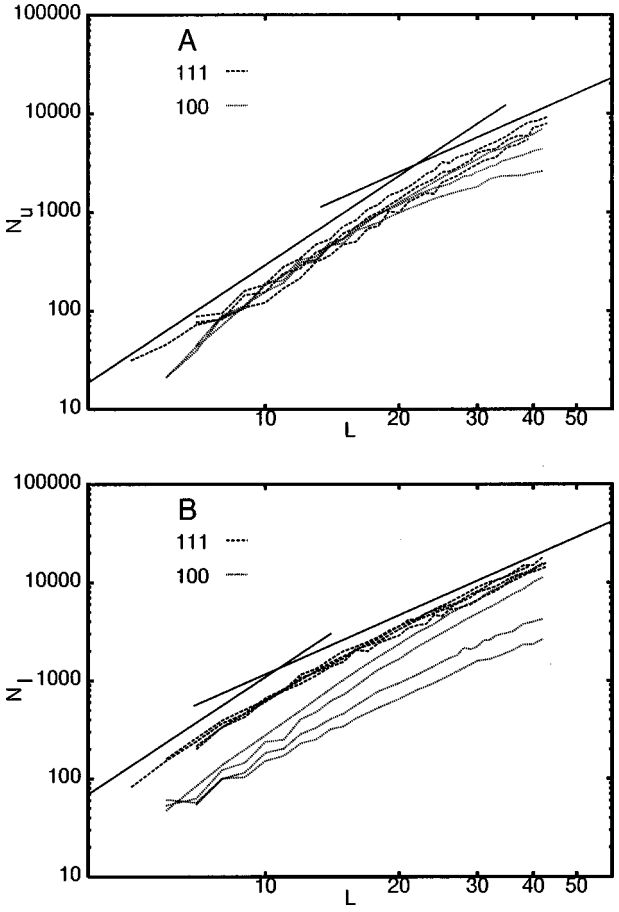

FIG. 3. The number of broken bonds in (A) the upper half of the cube, and (B) the lower half of the cube, plotted as functions of L. Results are shown for both the (100) and (111) directions, and for $a=5$, 13, 51, and 200. The full lines are functions proportional to $L^{3.0}$ and $L^{2.0}$.

To further investigate the dimension of the crack structures, we ''turned the cubes upside down'' and calculated the roughness (i.e., the variance of the width) of the crack surface after all loose fragments were removed. This was done for $a=4$ and 100 and $A=0.65$ and 1.0. We found that there is hardly any variation in the surface roughness as the size of the cube is changed (Fig. 4). This further supports the above suggestion that crack structures are simply two dimensional on a large scale. (Only for $a=100$ and $A=0.65$ is there some indication that roughness increases with the size L.)

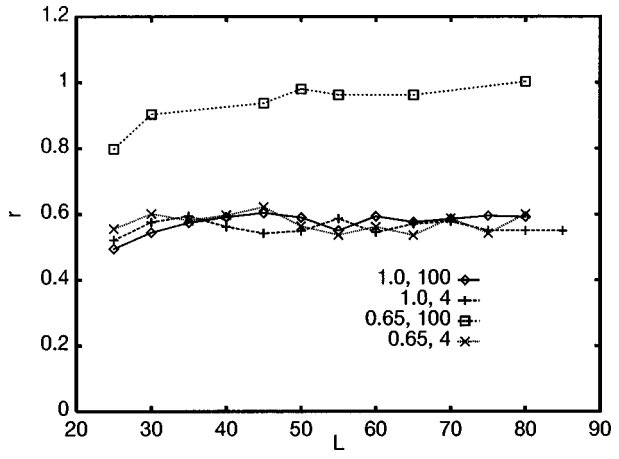

FIG. 4. The roughness of the top surfaces of the cubes as a function of their size L. Results are shown for $a=4$ and 100, and for compression wave amplitudes 0.65 and 1.3.

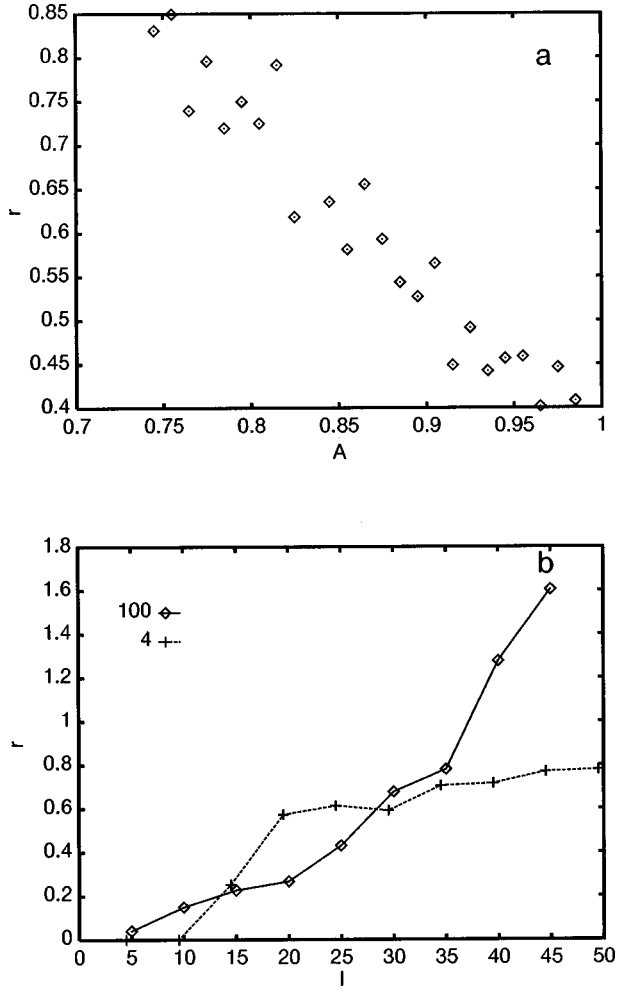

FIG. 5. (a) The roughness of the crack surface of the cubes as a function of the amplitude of the compression wave. (b) The roughness of the crack surface of the cubes as a function of the wavelength of the compression wave ($a=4$ and 100).

It is generally accepted that the self-affine crack structures in the quasistatic limit are created as a result of an interplay between quenched disorder trying to delocalize the fracture, and stress enhancement trying to localize the fracture. Stress enhancement is weaker in three dimensions than in two, which means that disorder more easily dominates over crack propagation, and a fairly large amount of bonds will be broken before crack propagation appears. This is especially true for a high amplitude of the compression wave. Then a large number of bonds are broken rapidly before the stress enhancement field at the crack tips has time to form. Disorder dominated fracture means that broken bonds are evenly distributed over a volume. It is, thus, not very suprising that the fracture structures are three dimensional on small scales in Fig. 3. Notice that the ''fracture structures'' of Fig. 3 are not the ''backbone'' of the cracks, but that all broken bonds are counted. The backbone may still have a fractal dimension [16], at least on small scales. For the backbone to be fractal on large scales, however, the amount of broken bonds would

have to be right at the point where cracks percolate, which is generally not the case for dynamic fracture. In a quasistatic case, fracture will cease the moment cracks percolate the cube, while, in a dynamic case, fracture will continue because of the kinetic energy. This effect is particulary strong for high amplitude impacts.

On a large scale, however, the fracture structures of Fig. 3 have a limited depth in the z direction. An examination of the simulations gave the following explanation for this. As already mentioned an important effect is that elastic energy is reflected and absorbed by cracks. If the amplitude of the compressive wave is, at some moment in time, high enough to instantly create extensive damage in a plane perpendicular to the propagation direction of the wave, the amplitude of the compression wave will decrease drastically. If the amplitude then becomes sufficiently low, no more cracks will be formed. This is what happens close to the bottom face of the cube for $a=100$, and close to the opposite face for $a=4$. Consequently, the fracture structures will have a limited depth in the propagation direction of the wave. In the other two directions there are no such limiting effects. The fracture structures will thus be two dimensional on a large scale. This effect is, of course, only valid at high loads (overload), for which extensive damage is rapidly formed close to the bottom or top faces of the cube. Right at the ''critical'' amplitude, at which fracture is just about initiated, the situation may be different. For dynamic fracture this critical amplitude is reminiscent in a way of quasistatic fracture, as only a few cracks will be initiated, which allows extensive crack propagation to appear. This results in an increasing roughness with decreasing amplitude of the compression wave [Fig. 5(a)]. Another way to approach the quasistatic limit is to increase the wavelength of the compressive wave. As demonstrated in Fig. 5(b), a longer wavelength means a higher surface roughness, which indicates a crossover to rough surfaces for quasistatic fracture. We also tried to find a power-law dependence of roughness on the size of the cube for the lowest possible amplitudes and the longest possible wavelengths, but this proved to be difficult. No better dependence than what is found in Fig. 4 for $a=0.65$ and $A=100$ could be found.

In summary, we have used a discrete numerical model to demonstrate that disorder controls the amount and location of damage resulting from an impact on a three-dimensional cube. For weak disorder, damage is mainly caused by constructive interference near the face opposite to the impact, while localization is the main mechanism that limits damage close to the impact for strong disorder. The crack structures formed in both these limits are three dimensional on a small scale and two dimensional on a large scale. As the quasistatic limit is approached the crack surface becomes more rough, which indicates a crossover to a self-affine surface.

[1] B. Khang, G. G. Batrouni, S. Redner, L. de Arcangelis, and H. J. Herrmann, Phys. Rev. B **37**, 7625 (1988).

[2] J. Åström and J. Timonen, Phys. Rev. E **55**, 4757 (1997).

[3] J. Åström and J. Timonen, Phys. Rev. Lett. **78**, 3677 (1997).

[4] L. Oddershede, P. Dimon, and J. Bohr, Phys. Rev. Lett. **71**, 3107 (1993).

[5] S. Zapperi, P. Ray, H. E. Stanley, and A. Vespignani, Phys. Rev. Lett. **78**, 1408 (1997).

[6] G. Hernandez and H. J. Herrmann, Physica A **215**, 420 (1995).

[7] F. Kun and H. J. Herrmann, Int. J. Mod. Phys. C **7**, 837 (1996).

[8] M. Marsili and Y.-C. Zhang, e-print, cond-mat/9606149.

[9] *Statistical Models for the Fracture of Disordered Media*, edited by H. J. Herrmann and S. Roux (North-Holland, Amsterdam, 1990).

[10] M. Sahimi and S. Arbabi, Phys. Rev. B **47**, 695 (1993); S. Arbabi and M. Sahimi, *ibid.* **47**, 703 (1993).

[11] This is a similar procedure to that in the standard finite element method.

[12] L. de Arcangelis, A. Hansen, H. J. Herrmann, and S. Roux, Phys. Rev. B **40**, 877 (1989).

[13] V. I. Räisänen, E. T. Seppälä, M. J. Alava, and P. M. Duxbury, Phys. Rev. Lett. **80**, 329 (1998); V. I. Räisänen, M. J. Alava, and R. M. Nieminen (unpublished).

[14] C. G. Batrouni and A. Hansen, Phys. Rev. Lett. **80**, 325 (1998).

[15] S. Arbabi and M. Sahimi, Phys. Rev. B **41**, 772 (1990).

[16] M. Sahimi, M. C. Robertson, and C. G. Sammis, Phys. Rev. Lett. **70**, 2186 (1993).